BOREAL ENVIRONMENT RESEARCH 18: 341–358
ISSN 1239-6095 (print) ISSN 1797-2469 (online)

Helsinki 27 September 2013

Modelling experiments on air–snow–ice interactions over Kilpisjärvi, a lake in northern Finland

Yu Yang[1)]*, Bin Cheng[1)2)], Ekaterina Kourzeneva[2)3)], Tido Semmler[4)5)], Laura Rontu[2)], Matti Leppäranta[6)], Kunio Shirasawa[7)] and Zhijun Li[1)]

[1)] *State Key Laboratory of Coastal and Offshore Engineering, Dalian University of Technology, Dalian 116024, China (*corresponding author's e-mail: yangyang-0606@hotmail.com)*
[2)] *Finnish Meteorological Institute, P.O. Box 503, FI-00101 Helsinki, Finland*
[3)] *Russian State Hydrometeorological University, Malookhtinsky pr. 98, 195196 St. Petersburg, Russia*
[4)] *Alfred Wegener Institute for Polar and Marine Research, Am Handelshafen 12, D-27570 Bremerhaven, Germany*
[5)] *Met Éireann, Glasnevin Hill, Dublin 9, Ireland*
[6)] *Department of Physics, P.O. Box 48, FI-00014 University of Helsinki, Finland*
[7)] *Institute of Low Temperature Science, Hokkaido, University, Kita-19, Nishi-8, Kita-ku, Sapporo, Hokkaido 060-0819, Japan*

Received 22 Dec. 2011, final version received 14 Dec. 2012, accepted 3 Dec. 2012

Yang, Y., Cheng, B., Kourzeneva, E., Semmler, T., Rontu, L., Leppäranta, M., Shirasawa, K. & Li, Z. J. 2013: Modelling experiments on air–snow–ice interactions over Kilpisjärvi, a lake in northern Finland. *Boreal Env. Res.* 18: 341–358.

The evolution of snow and ice thicknesses and temperature in an Arctic lake was investigated using two models: a high-resolution, time-dependent model (HIGHTSI) and a quasi-steady two-layer model on top of a lake model (FLake). *In situ* observations and a Numerical Weather Prediction model (HIRLAM) were used for the forcing data. HIRLAM forecasts, after orography correction, were comparable with the *in situ* data. Both lake-ice models predicted the ice thickness (accuracy 5 cm), surface temperature (accuracy 2–3 °C in winter, better in spring), and ice-breakup date (accuracy better than five days) well. HIGHTSI was better for ice thickness and ice-breakup date, while FLake gave better freezing date. Snow thickness outcome was worse, in particular for the melting season. Surface temperature was highly sensitive to air temperature, stratification and albedo, and the largest errors (positively biased) resulted in strongly stable conditions.

Introduction

Ice cover on large lakes is known to have an impact on the regional climate and weather. Freezing of a lake can significantly influence the heat exchange between air and the underlying waterbody, since snow and ice introduce a completely different surface for the thermal properties and roughness as compared with open water. In particular, the surface temperature of an ice-covered lake depends on the thicknesses of snow and ice. In the early ice growth season, the surface temperature can be much higher on lake ice than on land, and this not only influences the surface heat loss, but also the stability of the atmospheric stratification. During the melting season the surface temperature is controlled by the ice to remain at 0 °C.

During the recent decades, the ice cover of most Arctic lakes shows a trend toward later

Editor in charge of this article: Veli-Matti Kerminen

freeze-up and earlier ice breakup (Magnuson *et al*. 2000, Hodgkins *et al*. 2002, George *et al*. 2004, Lei *et al*. 2012). The course of ice season is largely controlled by air temperature, but ice decay time is also influenced by snow and ice accumulation during the winter, and solar radiation (Leppäranta 2009, Brown and Duguay 2010, Lei *et al*. 2011). Thus there is a local positive feedback from lakes to long-term atmospheric warming or cooling that makes lake ice an important factor in climate modelling (Brown and Duguay 2010).

Understanding the short-term interactions of lake ice and atmosphere is essential for the Numerical Weather Prediction (NWP). With the increase of the spatial resolution (up to 1 km presently) of mesoscale NWP models and data assimilation systems, the importance of lakes and lake ice will still increase (Mironov *et al*. 2010, Salgado *et al*. 2010, Eerola *et al*. 2010). There, the most important lake variables are the surface temperature and the state of the surface (open water/ice/snow). This brings the need to introduce parameterization schemes for snow and ice mass and heat balances in NWP models, such as the High Resolution Limited Area Model (HIRLAM) (Undén *et al*. 2002), which is studied in this work. The initial temperature and state of the lake surface can be derived from real-time satellite data, but *in situ* measurements or model hindcasts are needed for the snow and ice thicknesses.

Historically, time-dependent heat conduction models and quasi-steady heat-flux models have been used in lake-ice thermodynamics investigations. The former category solves the thermal diffusion equation in snow and ice (e.g., Croley and Assel 1994, Leppäranta and Uusikivi 2002, Leppäranta 2009, Yang *et al*. 2012), whereas the latter category solves the quasi-steady heat flux through 1–3 snow and ice layers (e.g., Leppäranta 1983, Hostetler *et al*. 1993, Goyette *et al*. 2000, Mironov 2008). The difference between these model categories is that quasi-steady models ignore the heat capacity and, in practice, time-dependent models have a higher vertical resolution.

The present lake-ice modelling work is based on the time-dependent, high-resolution model HIGHTSI (Launiainen and Cheng 1998) and the lake model FLake (Mironov *et al*. 2010) which has a quasi-steady two-layer ice model on top. Two major issues concerning these models are examined: (1) the sensitivity to atmospheric forcing, and (2) the feasibility to couple with NWP models for improvement of weather forecasting. The first part is a continuation to Semmler *et al*. (2012), who studied the sensitivity of HIGHTSI and FLake to thermal properties of snow and ice. The research focus was on the influence of the accuracy of the forcing data on the accuracy of the simulated snow and ice thicknesses and surface temperature. The model experiments were performed for Kilpisjärvi, a lake located in Finnish Lapland (69°03´N, 20°50´E). The results showed that improvements to produce the freezing and ice-breakup dates can be introduced into both models. Comparisons between the measured and modelled surface temperatures confirmed that these models could essentially improve the surface boundary condition of NWP models and consequently the quality of local weather forecasting.

Numerical lake ice models

General

Thermodynamic lake-ice models contain ice and snow layers. They are one-dimensional (vertical), forced by solar heating, air–ice/snow heat exchange, and heat flux from the waterbody to ice (e.g., Leppäranta 2009). The models are based on the heat diffusion law with solar radiation as a source term and with moving vertical boundaries to account for the changes in the thicknesses of snow and ice. Snow accumulation is an external input, whereas ice grows when the latent heat released during ice growth can be conducted through the ice and snow to the atmosphere. The melting of snow and ice results from surface heat fluxes and penetration of solar radiation into snow and ice. The most sensitive factors are snow accumulation and albedo (Yang *et al*. 2012).

Lake-ice models differ in the treatment of the heat capacity of ice, parameterization of air–ice heat fluxes and albedo, treatment of snow physics, and numerical technology. When the heat capacity is ignored, the temperature profile

is set immediately to a steady-state form corresponding to boundary conditions. Then, with the boundary conditions changing with time, a new steady-state profile is obtained at each time step. These kinds of models can be called quasi-steady models. They have also been called non-inertial models because ignoring the heat capacity means that there is no thermal inertia. Correspondingly, with a finite heat capacity we have models with thermal inertia.

Lake-ice models can provide the temperature and state of the surface but not the actual surface roughness. The surface temperature is quite a delicate model variable as it responds fast to external heat fluxes (*see* Leppäranta and Lewis 2007). Resolving the surface temperature in time scales of hours necessitates the inclusion of heat capacity and high vertical resolution. Quasi-steady models can produce the surface temperature over much longer time scales. Two ice models are considered here: a stand-alone, time-dependent, high-resolution model (HIGHTSI) and a quasi-steady, two-layer (ice + snow) model which forms the top of a lake model (FLake). A detailed comparison of the model physics is given in Appendix.

Time-dependent, high-resolution model HIGHTSI

HIGHTSI (Launiainen and Cheng 1998, Cheng *et al*. 2003 and 2008) solves the heat conduction equation for the snow and ice layers, for the evolution of ice and snow temperature and thickness. At the upper boundary, shortwave and long-wave radiative fluxes and turbulent heat fluxes are parameterized, with the turbulent fluxes taking into account the stability of atmospheric stratification. Alternatively, these fluxes are taken from an atmospheric model. The surface temperature is solved from the surface energy balance that couples the snow and ice sheet with the atmosphere. At the bottom of the ice sheet, the heat and mass balance is controlled by freezing and melting and prescribed heat flux from the water, which is currently taken as a constant equal to 1.5 W m^{-2}. The level of heat flux is to some degree lake-specific, and here the cited value was obtained by model calibration. The snow thickness and density are modelled from precipitation, wind and temperature (packing), snow-ice formation (sink), and surface and internal melting (Cheng *et al*. 2003). The formation of snow ice is a source for the ice layer (Saloranta 2000, Cheng *et al*. 2006, 2008). The thermal conductivity of snow is parameterized based on density (Sturm *et al*. 1997).

HIGHTSI was adapted for lake-ice investigations by Yang *et al*. (2012). The model has a high vertical resolution containing normally 10 snow layers and 20 ice layers. 'High resolution' refers to the requirement that daily cycles in the temperature evolution can be resolved. The time scale of heat diffusion in ice is $\tau \sim L^2/D = 10(L/\mathrm{m})^2$ days, where D is the heat diffusion coefficient and L is the vertical length scale. For $L \sim 0.1$ m, we have $\tau \sim 0.1$ days, which is approximately the time-step needed for daily cycles in numerical modelling. With the combined ice and snow thicknesses of 1 m, this means ~10 grid cells.

Quasi-steady, two-layer model FLake

FLake simulates all-year lake temperature profiles based on the heat and kinetic energy budget with a sediment layer beneath and, in winter, ice and snow layers on top (Mironov 2008, Mironov *et al*. 2010). The upper water layer is mixed and the lower water layer is stratified, taken as the thermocline which is described using an assumed self-similar profile structure. This structure is also used to describe the temperature profile of the thermally-active upper layer in the bottom sediment and in the ice and snow sheet. FLake is intended for use as a lake parameterization scheme in Numerical Weather Prediction (NWP) and climate models. Here FLake with the parameterization scheme 'sensitivity experiment 3' of Semmler *et al*. (2012) was taken (thermal conductivity of snow and the albedo have been modified from the original FLake).

FLake simulations were performed in two modes. First, a stand-alone configuration was taken as typically used for FLake development and validation. The second mode was to take it as the lake module in the SURFace EXternalized surface model (SURFEX) (Salgado *et al*. 2010,

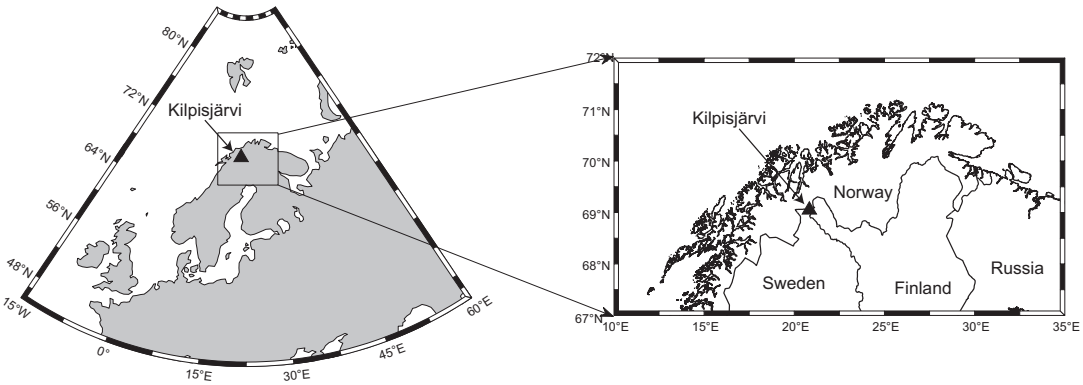

Fig. 1. Location of Kilpisjärvi (triangle) (69°03´N, 20°50´E).

Le Moigne 2009), one of the typical environments in FLake applications. SURFEX includes FLake along with other modules for land, sea and urban areas, and it also allows two-dimensional simulations. We performed one-dimensional simulations with an assumed lake fraction of 100% and other modules switched off.

Model study

Snow and ice measurements

Kilpisjärvi is a lake located in the northwest corner of Finnish Lapland, at 69°03´N, 20°50´E (Fig. 1). The lake surface area is 37.1 km^2, with an average depth of 19.5 m. The lake is located in the Scandinavian Mountains at an elevation of 473 m above sea level. The average ice season lasts 7.3 months (from 9 November to 18 June), and the ice thickness reaches its maximum value (75–115 cm) in April (Lei *et al*. 2012). Snow and ice measurements have been carried out by Kilpisjärvi Biological Station (KBS) since 1952. The data are archived in the Hertta database of the Finnish Environment Institute (http://www.ymparisto.fi/default.asp?node=14812&lan=en).

In the winter 2007–2008, snow and ice thicknesses were measured at every 10 m along a 100-m section in the near-shore zone at 10-day intervals. The measurements were averaged for the mean snow and ice thicknesses of each measurement day. The maximum thickness of snow (36 cm) and ice (85 cm) were recorded at the end of April. The freezing and ice-breakup dates were 14 November 2007 and 21 June 2008, respectively, both within five days from the long-term average. The freezing date is defined as the first day when no open water is found in the visible range from the site, and the ice-breakup date refers to the final disappearance of the ice from the visible range. The snow thickness on the ground was measured twice a day at the Kilpisjärvi Weather Station (69°02´N, 20°47´E, WMO station 28010, Enontekiö-Kilpisjärvi Kyläkeskus, henceforth EKK) in the vicinity of Kilpisjärvi.

A joint Finnish–Japanese winter experiment was carried out in Kilpisjärvi in the winter 2007–2008 (Leppäranta *et al*. 2012). An automatic ice station 'Lotus' (a floating raft) was active from 14 December 2007 to 12 June 2008. The data provided the surface radiative temperature, which was detected by an infrared thermosensor (THI-303N, Tasco Ltd., Japan) with the accuracy of 0.3 °C. Incoming and outgoing solar radiative fluxes at ice surface were monitored by pyranometers (CM3, PCM-03H, Kipp & Zonen, Holland). The snow depth on lake ice was measured using a sonic ranging sensor (SR50M-45, Campbell Scientific, Canada). The original data were sampled at every 20 minutes, and they were averaged to one-hour intervals for our study. The sensor readings showed that the seasonal maximum snow thickness was 50 cm at the end of March and that the lake was free of snow at the end of May (Fig. 2).

The KBS and EKK snow stakes provided snow accumulation on land (KBS was close to the lake shore). The snow thickness showed

similar variability but the EKK values reached a much higher level (maximum 90 cm) than those of 'Lotus' and KBS (50 cm). However, several accumulation events in 'Lotus' data (e.g. 27–30 January, 13–15 February and 16–17 April) were well correlated with the EKK time series (EKK gave 19.4 mm, 33.6 mm and 7.3 mm precipitation for these periods, respectively). The KBS snow-thickness record showed much smoother variation in comparison with the 'Lotus' high-resolution data, but the level of snow thickness was closer, and therefore the KBS snow thickness was more representative than the EKK snow thickness for the snow accumulation on the lake ice.

The ice grew gradually from mid-November until the end of March, and the mean growth rate was 0.6 cm d^{-1} (Fig. 2). This was followed by a sustainable snow-ice growth in April, and the maximum ice thickness became 85 cm when the snow depth reached 36 cm. The corresponding long-term averages are 89 cm and 38 cm, respectively (Lei *et al*. 2012). Ice melting started after the onset of snow melting at the end of April. When the snow had disappeared, ice melting was accelerated and the average ice melt-rate was 1.4 cm d^{-1}. The melting season lasted for almost two months, until 21 June (Leppäranta *et al*. 2012).

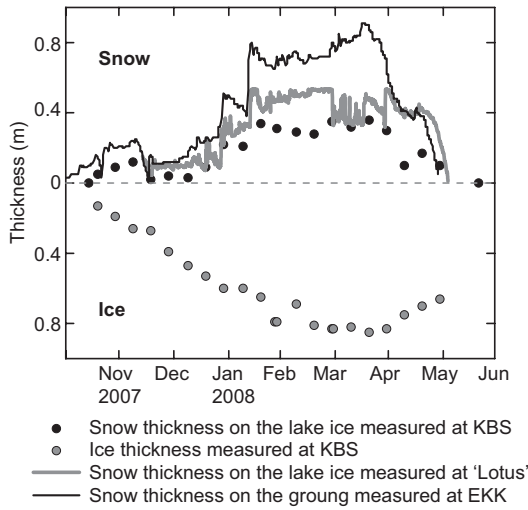

Fig. 2. Snow and ice thickness measurement results. The zero level represents the snow–ice interface.

Atmospheric forcing

Modelling experiments were performed with two types of forcing data: local weather station (EKK), and the NWP model (HIRLAM). The local weather data were recorded every three hours for temperature, humidity, wind and cloudiness, whereas the accumulated precipitation was measured every 12 hours. All the data were interpolated to one-hour interval for the model experiments. The radiative fluxes were parameterized by simple schemes (*see* Table 1).

For the HIRLAM forcing, the lowest model level (ca. 30 metres above the surface) forecasts of air temperature, humidity, wind, radiation fluxes and snowfall were employed. This level represents the surface conditions, but at times the outcome can be biased to represent the surface conditions as normally understood (2-m level for the temperature and humidity and 10-m level for the wind). Comparisons between HIRLAM and EKK data are important also in providing information about the quality of the HIRLAM 'surface' data. The data of the HIRLAM grid point nearest to Kilpisjärvi was taken from the archive of the Finnish Meteorological Institute. The horizontal grid-size was ca. 17 km. The forcing data represent a series of 3–6 h forecasts, initialized four times a day and interpolated to one-hour intervals.

For both types of forcing data, the turbulent fluxes were calculated by HIGHTSI and FLake including the influence of the stability of atmospheric stratification. There was an orographic difference between the real altitude of Kilpisjärvi (473 m) and the altitude of the corresponding HIRLAM grid point (721 m). An adiabatic (–0.0065 K m^{-1}) correction was applied to the air temperature, relative humidity was assumed constant, and surface pressure was adapted using the hydrostatic approximation. Measured and HIRLAM atmospheric variables are compared in Fig. 3 (for monthly-mean values *see* Table 1). This comparison allows us to make a quantitative assessment of the HIRLAM results.

The HIRLAM wind speeds were in line with the measurements. Minimum values, however, seemed to be overestimated, and the monthly average was greater than the measured one. The HIRLAM air temperature caught the observa-

Table 1. The monthly averages atmospheric conditions at Kilpisjärvi from weather station EKK and HIRLAM. Q_s and Q_d are incoming shortwave and long-wave radiative fluxes, respectively. Note: The Q_s and Q_d, values presented here are results from internal HIGHTSI parameterizations and from HIRLAM simulations. The HIRLAM air temperature (T_{air}) presented here contain orography correction.

	Wind (m s^{-1})		T_{air} (°C)		Prec. (mm month^{-1})			Q_s (W m^{-2})			Q_d (W m^{-2})	
	EKK	HIRLAM	EKK	HIRLAM	EKK total	HIRLAM total	HIRLAM snow	EKK platform measured	EKK (Shine 1984, Bennett 1982)	HIRLAM	EKK (Efimova 1961, Jacobs 1978)	HIRLAM
September	4.0	5.1	4.4	4.1	59.0	104.7	0.1	–	71.0	46.0	322.4	296.8
October	4.0	6.3	2.8	2.7	32.4	97.3	31.0	–	21.0	17.0	316.2	291.6
November	3.9	5.2	–5.9	–5.0	34.0	54.2	43.9	–	1.1	1.8	272.5	257.1
December	4.4	7.1	–5.0	–3.7	32.3	92.0	35.2	0.1	0	0	275.4	264.9
January	4.0	6.4	–8.8	–7.2	39.5	41.4	28.3	1.3	0.2	2.9	256.7	243.5
February	4.6	7.0	–8.0	–6.9	68.5	87.9	63.9	15.2	10.8	16.1	262.7	247.4
March	2.2	4.4	–12.3	–8.1	29.8	31.4	28.4	67.6	58.2	77.0	240.9	236.0
April	4.3	5.5	–4.4	–3.1	39.4	65.7	55.4	123.9	159.1	141.3	275.7	263.6
May	3.7	4.5	1.7	1.9	21.4	80.9	30.7	209.2	189.2	191.7	302.2	276.6
June	3.8	4.1	6.9	6.8	54.3	98.4	2.6	222.0	214.0	189.5	336.4	299.6

Fig. 3. (**a**) Wind speed (V_{air}), (**b**) air temperature (T_{air}), and (**c**) total precipitation (Prec.) measured at the EKK weather station and HIRLAM simulated for the grid nearest to EKK.

tions quite well. In general, for autumn and early summer HIRLAM gave almost unbiased temperatures (Table 1) when the atmospheric boundary layer was normally neutrally stratified. But for winter months, low temperatures in particular were overestimated, and the bias was 4.2 °C for the monthly-mean value in March. This was likely due to a stable stratification and inversion in the atmosphere, a typical bias condition in NWP models (Hanna and Yang 2001, Järvenoja 2005). The HIRLAM monthly precipitation was generally greater than the measured one, particularly in autumn and spring, but the HIRLAM snowfall corresponded well to the EKK precipitation. The precipitation was assumed to be solid when the screen-level temperature fell below 0.5 °C.

Unfortunately, no radiative fluxes were available from the EKK weather station. The solar-radiation flux was measured at the 'Lotus' station after the polar night from the end of January onwards. The formulae by Shine (1984) and Bennett (1982) matched the measurements better than HIRLAM (*see* Fig. 4), especially when the radiation level was < 400 W m^{-2}. Between February and June 2008, the solar radiation was generally underestimated by the HIRLAM and HIGHTSI parameterizations (*see* RMSE values in Fig. 4).

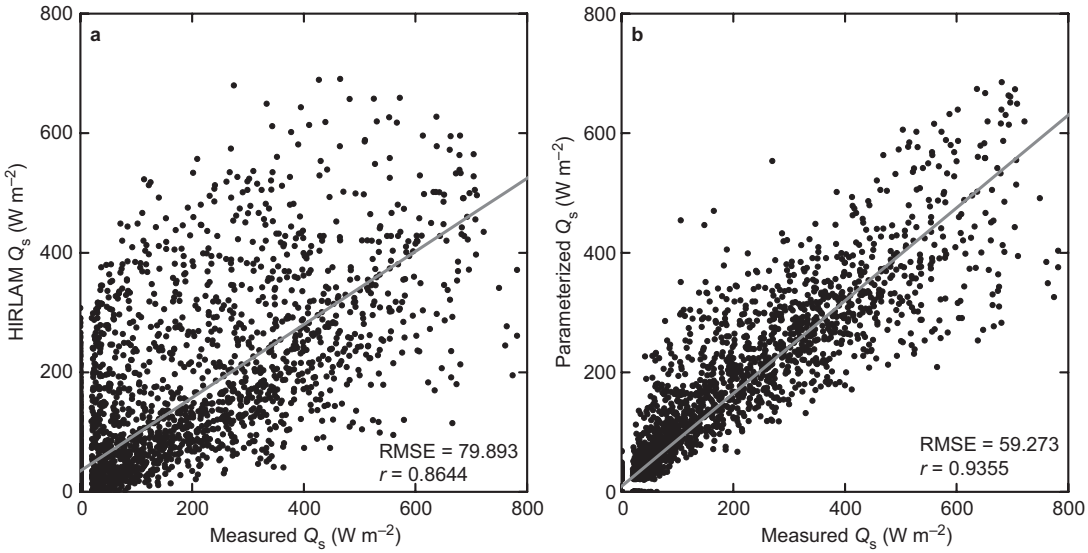

Fig. 4. Incoming solar radiation: (**a**) measured and HIRLAM forecast, and (**b**) measured and parameterized by Shine (1984) and Bennett (1982) formulae. The data cover the period from January to June 2008.

For the incoming long-wave radiation, HIRLAM gave systematically smaller values as compared with the standard parameterization schemes based on temperature, cloudiness and humidity (Table 1). The difference was 11 W m^{-2} in December–March and 23 W m^{-2} in September–November and April–June. The average difference for the whole ice season was 17 W m^{-2}. In the summer, there were more uncertainties, e.g. due to water vapour in the atmosphere.

The starting date for the models was 1 September. HIGHTSI was initialized with thin ice (0.02 m) and uniform ice temperature (–0.25 °C). The thickness and temperature were kept as such until the ice started to grow continuously. This was taken as the freezing date. FLake was started with a uniform temperature (4 °C) in the entire water column corresponding to the autumn turnover. The average depth of Kilpisjärvi is 20 m.

Results

Six 'Model & Forcing' experiments were performed (Table 2). Orographic correction was made in HIRLAM cases except, for comparisons, in M3F2.

In practice, the configuration differences between SURFEX-FLake and Standalone FLake were merely technical leading to the results of M2F1 and M3F1 close to each other. These simulations confirmed that the technical differences did not lead to significantly different results. Only the M3F1 results are included in the following sections. The influence of orography corrections to HIRLAM data was investigated by using SURFEX-FLake and Standalone FLake together.

Snow and ice thicknesses

The snow accumulation events were generally well reproduced by M1F1, except for May

Table 2. Model experiments carried out in this study.

Model	External forcing	Experiment
HIGHTSI (M1)	EKK (F1)	M1F1
	HIRLAM* (F2)	M1F2
SURFEX-FLake (M2)	EKK (F1)	M2F1
	HIRLAM* (F2)	M2F2
Standalone FLake (M3)	EKK (F1)	M3F1
	HIRLAM** (F2)	M3F2

* the orography correction is taken into account.
** without orography correction.

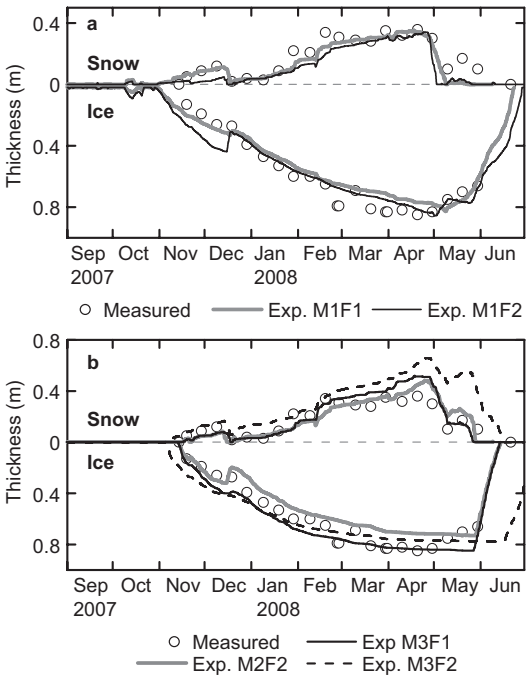

Fig. 5. Influence of the forcing data on the models. Snow and ice thickness from (**a**) HIGHTSI M1F1 (EKK) and M1F2 (HIRLAM); and (**b**) SURFEX-FLake M2F2 (HIRLAM) and Standalone FLake M3F1 (EKK) and M3F2 (HIRLAM). The circles are the measured snow or ice thickness. The zero level is the snow–ice interface.

(Fig. 5). The errors seemed to be resulting from the EKK precipitation. The modelled snow melting in early winter and late April was in agreement with the measurements, as were the ice thickness and the onset of melting.

In the M1F1 experiment, the HIGHTSI freezing date was 2 November while the observation was 14 November. The HIGHTSI treatment of the freezing date is inaccurate (Yang *et al*. 2012), because the model does not include an active waterbody. The modelled ice-breakup date (22 June) was very close to the observation (21 June). The experiment M1F2 yielded the snow thickness comparable with M1F1 for most of the winter season but it was underestimated for early winter. The snowfall modelled by HIRLAM was in November (43.9 mm) and December (35.2 mm) larger than that recorded at EKK (33.8 mm and 19.2 mm). However, the higher HIRLAM temperature resulted in faster snow melting in April in M1F2 as compared with that in M1F1 (Table 1). Differences in modelled ice thickness between the experiments M1F1 and M1F2 appeared again in the early and late winter. In M1F1, faster ice growth in the early winter was associated with less snow accumulation, and the resulting ice-breakup date was 22 June, eight days earlier than that in M1F2. The EKK and HIRLAM air temperatures were approximately the same in June. The delayed ice-breakup date may result from smaller incoming shortwave and longwave radiation in HIRLAM in June.

The freezing dates in the experiments M2F2 and M3F1 were about the same and very close to the recorded one. The ice-breakup dates were earlier than the recorded one. The snow depth affected directly the onset of ice melting. There was snow still left in May in M2F2 due to the combined effect of higher snow accumulation (Fig. 3c) and colder air in the HIRLAM data (Fig. 3b) as compared with that in the EKK forcing. The modelled snow and ice thicknesses followed the measurements reasonably well. The maximum snow thickness was slightly overestimated that is probably due to the constant snow density used.

The original HIRLAM air temperature (altitude 721 m) was approximately 1.6 °C smaller than the air temperature at the lake surface (altitude 473 m). Without the orography correction, more precipitation fell in solid phase leading to the overestimation of the snow thickness and consequently to the underestimation of the maximum ice thickness by about 5 cm. The freezing date was 4 November, nine days earlier than in the experiment M3F1. The large, overestimated snow depth caused a dramatically-postponed ice-breakup date.

The choice of the external forcing (EKK or HIRLAM) did not significantly alter the snow thickness in the HIGHTSI experiments M1F1 and M1F2 or in the FLake experiments M2F2 and M3F1. The smaller snow water equivalent in the EKK data (248 mm) than in the HIRLAM forecasts (320 mm) and the slightly lower average air temperature in EKK than in HIRLAM led to compensation of the errors (Table 3).

Surface temperature analysis

The different external forcing and model phys-

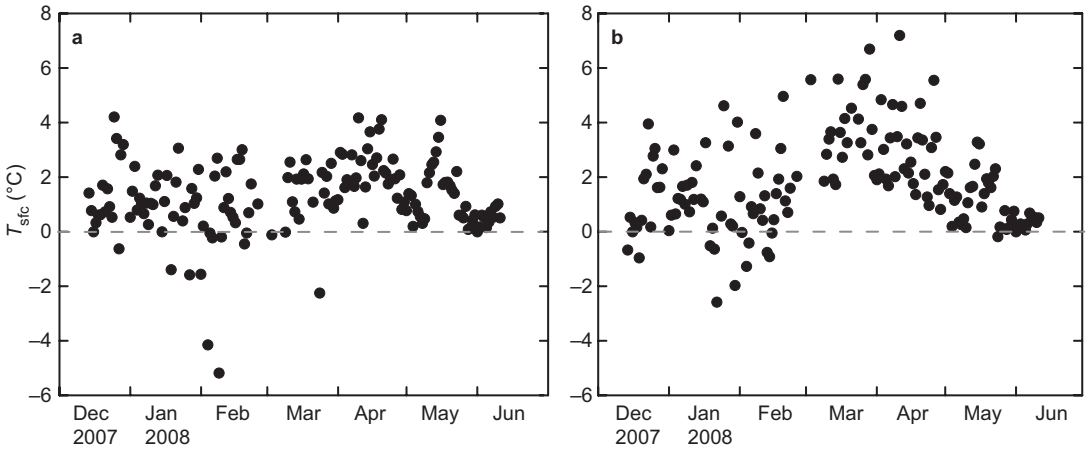

Fig. 6. Daily mean-surface temperature differences (**a**) between calculated by HIGHTSI and measured at EKK (experiment M1F1), and (**b**) between calculated by HIGHTSI and HIRLAM (experiment M1F2).

ics gave direct impact on the modelled surface temperature. For the sake of clarity, the experiments M1F1 and M1F2 (HIGHTSI/EKK and HIGHTSI/HIRLAM) were used to examine the impact of external forcing while the experiments M1F1 and M3F1 (HIGHTSI/EKK and FLake/EKK) were used to evaluate the impact of the model physics.

The HIGHTSI daily mean surface temperature, with both forcings, showed a positive bias for most cases (Fig. 6). Compared with M1F1, M1F2 had large surface temperature errors in March and April when the HIRLAM monthly-mean air temperatures were 4.2 °C and 1.3 °C higher, respectively, than those measured at EKK (*see* Table 2). This could partly be due to the usual bias of the model surface temperature towards higher temperature in stable situations.

The hourly surface temperatures for the experiments M1F1 and M3F1 had positive biases, differences being mainly within the range –5 to +10 °C in M1F1 and –10 to +10 °C in M3F1 (Fig. 7). The large positive bias was likely connected to the strongly-stable atmospheric boundary layer (*see* Table 4 for the cases when the difference was more than 5 °C).

The large differences occur mostly during the night when the surface is much colder than air, air is cold and wind is weak, as is typical for a strongly stable stratification (*see* Table 4). The errors in the monthly-mean modelled surface temperature are summarized in Table 5. In cold periods (early winter), RMSE was around 2 °C in both model runs, increasing to some extent in the early spring and decreasing towards the early summer. Overall, the experiment M1F1 yielded a slightly better surface temperature as compared with M3F1 (bias 1.65 °C *versus* 1.87 °C, and RMSE 2.31 °C *versus* 2.61 °C, respectively).

In order to better understand the errors in the

Table 3. The statistical analysis of simulated snow (h_{snow}) and ice (h_{ice}) thicknesses compared to observations.

Parameter	HIGHTSI				SURFEX-FLake		Standalone FLake			
	Exp. M1F1		Exp. M1F2		Exp. M2F2		Exp. M3F1		Exp. M3F2	
	h_{snow}	h_{ice}	h_{snow}	h_{ice}	h_{snow}	h_{ice}	h_{snow}	h_{ice}	h_{snow}	h_{ice}
Bias (cm)	–3.16	–2.12	–5.67	2.27	0.40	–6.32	1.74	5.41	13.86	6.19
Absolute error (cm)	3.94	6.97	5.81	7.29	4.97	7.71	5.70	6.15	13.86	11.08
RMSE (cm)	5.76	8.10	7.58	10.41	6.22	9.25	7.46	7.56	18.15	16.15
r	0.92	0.97	0.91	0.97	0.91	0.98	0.94	0.98	0.80	0.87

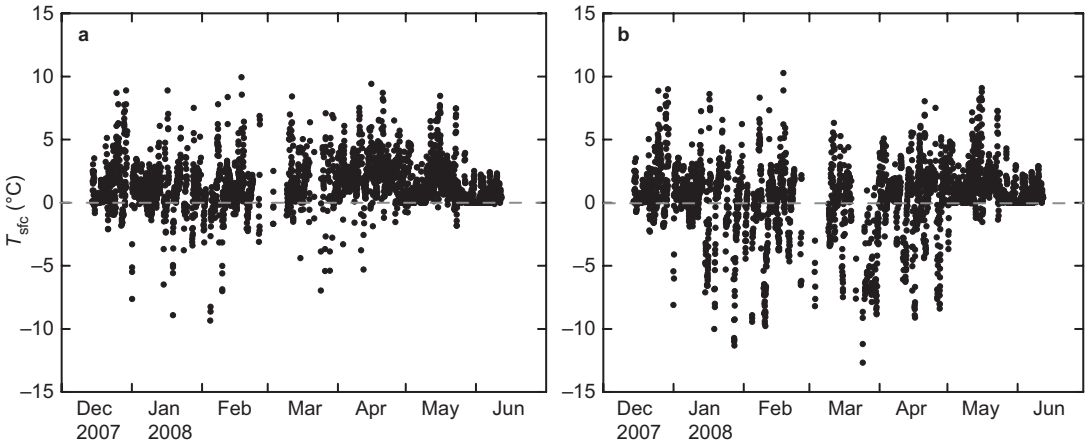

Fig. 7. Surface temperature (T_{sfc}) differences (**a**) between calculated by HIGHTSI and measured at EKK (experiment M1F1), and (**b**) between calculated by Standalone FLake and measured at EKK (experiment M3F1). All data (1-h interval) were included.

modelled surface temperature, we investigated the time series for a few selected periods in more detail. In a cold period (December), HIGHTSI and FLake produced quite similar surface temperatures (Fig. 8a). In the early winter, ice grew fast and the episodes of temperature increase were modelled reasonably well by both models (21, 23 and 27 December). The surface boundary layer was mostly neutral, and the turbulent fluxes were obtained correctly. The decrease in the surface temperature was underestimated for 23 and 28 December during a cold and stable boundary-layer situation. From 24 to 26 December, the decrease in the air temperature was perhaps associated with the surface inversion that made the surface temperature simulation very chal-

Table 4. Analysis of the cases in which the temperature difference was more than 5 °C. T_{air} = air temperature and T_{sfc} = surface temperature.

Condition	Time	Temperature difference	Cold	'Calm'
	18:00–06:00	$T_{air} - T_{sfc} > 5$ °C	$T_{air} < -5$ °C	$V_{air} < 3$ m s^{-1}
Exp. M1F1	60%	70%	57%	60%
Exp. M3F1	75%	53%	47%	57%

Table 5. Comparison of measured and calculated monthly-mean surface temperatures (T_{sfc}, °C).

	Measured monthly-mean T_{sfc}	Exp. M1F1					Exp. M3F1				
		Calculated T_{sfc}	Bias	Absolute error	RMSE	*r*	Calculated T_{sfc}	Bias	Absolute error	RMSE	*r*
December	–4.15	–2.70	1.45	1.67	2.49	0.86	–2.78	1.37	1.64	2.47	0.84
January	–7.90	–6.61	1.29	1.60	2.18	0.80	–7.32	0.58	2.10	2.89	0.58
February	–7.25	–6.02	1.23	1.65	2.35	0.80	–7.32	–0.07	2.31	3.16	0.59
March	–7.43	–5.29	2.14	2.25	3.19	0.87	–8.29	–0.87	2.90	3.84	0.79
April	–5.99	–3.55	2.44	2.48	3.07	0.88	–5.22	0.77	2.17	2.92	0.76
May	–2.17	–0.81	1.36	1.39	2.07	0.87	–0.84	1.33	1.40	2.15	0.78
June	–0.56	–0.05	0.51	0.51	0.80	0.57	–0.02	0.53	0.53	0.85	0.32
Mean	–5.06	–3.57	1.48	1.65	2.31	0.89	–4.54	0.52	1.87	2.61	0.82

lenging. Variations in the measured surface temperature were just responses to the variations in the air temperature. A thin snow cover may have also contributed to the similarity of HIGHTSI and FLake results.

The results of the surface temperature validation for February produced by HIGHTSI and FLake diverged from each other (Fig. 8b). There was a large difference on 10–12 February after a cold and stable boundary-layer situation (8 February), when both HIGHTSI and FLake again overestimated the surface temperature. The warming from 10 to 12 February was produced by HIGHTSI quite well, whereas FLake gave larger errors. The sensible heat flux increased in HIGHTSI drastically in response to the increase in the air temperature. Since HIGHTSI and FLake heat fluxes were nearly the same (*see* section 'Snow and ice thicknesses' above), the error in the FLake surface temperature was caused by ignoring the heat capacity or by the low vertical resolution. In April, the incoming solar radiation became strong (Fig. 8c). Both modelled surface-temperatures reacted clearly to this, and the overall value was higher in HIGHTSI than in FLake, both being higher than the measurements. The difference between the models as well as between the models and the measurements could have been caused by differences in the surface albedo, model vertical resolution or snow conditions.

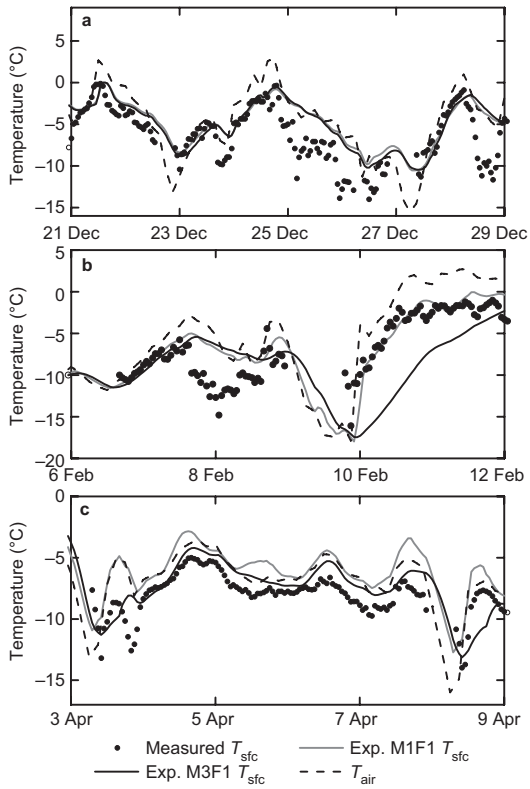

Fig. 8. Time series of surface temperatures measured at the 'Lotus' station and calculated by HIGHTSI and FLake surface temperatures for (**a**) December, (**b**) February and (**c**) April. The model runs were made using the EKK external forcing. The air temperature of the forcing is also shown.

In both models, the errors in the surface temperature resulted mainly from a too slow response. Firstly, technical reasons are possible. FLake takes the solar radiation as a pure surface forcing, which is too crude when solar radiation is strong and its penetration into the snow and ice provides immediate warming. HIGHTSI allows this penetration, but its implicit numerical scheme may produce a phase error (however, this has not been examined in earlier model applications). Secondly, inaccuracies in the forcing may have been the reason for the slow response. In stable conditions, turbulent fluxes are difficult to evaluate, and the standard methods to calculate the long-wave atmospheric radiative flux are inaccurate.

A proper way to determine the surface temperature is an iterative procedure. In the NWP community, however, simplified methods are often used due to computational cost requirements. A sensitivity HIGHTSI run with an approximate method to determine the surface temperature indicated that the difference (bias or RMSE) increased by 0.3–0.4 °C as compared with the HIGHTSI standard simulation (M1F1).

Model run with simplified snow conditions

The role of snow was studied by running HIGHTSI and FLake ignoring snow, and including the snow thickness recorded at EKK. Since snowfall was not included in the heat balance, neglecting snow had no impact on the modelled freezing date, but the modelled ice thicknesses were greater because the snow insulation was excluded from the simulation (Fig. 9).

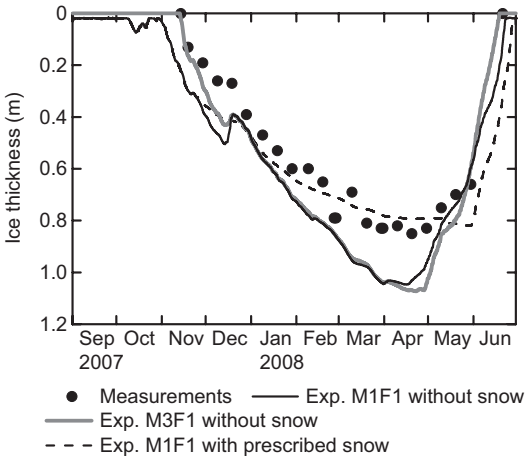

Fig. 9. Ice thickness modelled by HIGHTSI and Standalone FLake without taking snow into account. The external forcing are the measurements at EKK.

Without snow, HIGHTSI and FLake produced quite similar ice thicknesses between January and March, but in the melting season there were small differences. HIGHTSI produced almost the same ice-breakup date (23 June) as with snow (22 June) due to the error compensation: ice grew too fast in the growth phase because of the missing snow, and the too thick ice cover needed more days to melt. Also FLake yielded a delayed ice-breakup date (19 June) in the no-snow case as compared with the snow case (13 June). FLake tended to give a slightly thicker ice, and more time was needed to reach the ice-free state although FLake still melted the ice faster than HIGHTSI. When prescribing the snow, the thickness of ice was more realistically simulated but the onset of melting happened too late leading to a delayed ice-breakup date.

In the modelled snow cases, the errors in ice thickness and surface temperature were small as compared with the other cases (Table 6). With the prescribed snow, the errors were smaller than in the no-snow cases but larger than those with snow simulated by HIGHTSI. As compared with modelled snow cases, in the no-snow cases the mean errors in the modelled surface temperature were higher by 0.1–0.2 °C in HIGHTSI and 0.3–0.4 °C in FLake (*see* Table 6).

From the point of view of the surface heat balance, the major difference between the snow and bare ice surface is the different heat capacity and conductivity. In cold conditions, the longwave radiative and sensible-heat fluxes dominate the surface heat balance. When the sensible heat flux is strong, the surface temperature of snow and bare ice should not differ much from each other. In spring, solar radiation plays the key role in the surface heat balance. The differences between the albedo and extinction coefficient between ice and snow are large, and bare ice warms faster than snow-covered ice. When the surface is in the melting stage, the temperature is 0 °C. A closer look into the simulations suggested that the surface temperature error tended to be large in spring in the case without snow.

Freezing and ice-breakup dates

HIGHTSI yielded an early freezing date when using both the EKK and HIRLAM forcings.

Table 6. Differences between modelled measured snow and ice thicknesses and surface temperatures.

	Exp. M1F1			Exp. M3F1	
	with snow	prescribed snow	without snow	with snow	without snow
Ice thickness					
Bias (cm)	–2.12	6.17	14.06	5.41	12.41
Absolute error (cm)	6.97	9.80	14.64	6.15	13.03
RMSE (cm)	8.10	11.88	15.98	7.56	14.55
r	0.97	0.97	0.96	0.98	0.97
Surface temperature					
Bias (°C)	1.34	1.35	1.47	0.82	1.21
Absolute error (°C)	1.34	1.35	1.47	1.35	1.69
RMSE (°C)	1.65	1.65	1.89	1.81	2.15
r	0.95	0.95	0.91	0.86	0.81

The driving force of its simple procedure is the weather. In late autumn, EKK and HIRLAM air temperatures are close to each other, and thus the resulting freezing dates are almost the same. Early freezing is due to ignoring the heat storage of the waterbody. The HIGHTSI freezing date follows from switching into a negative heat balance for a given thin, initial, artificial ice layer that actually provides the earliest possible freezing of very shallow water. A previous study showed a high correlation between the air temperature and freezing date for Finnish lakes (Palecki and Barry 1986). More recently, Lei *et al*. (2012) showed that for Kilpisjärvi the freezing date is correlated with monthly mean air temperature between 15 October and 15 November. Since the cooling of the lake is forced by turbulent and long-wave radiation heat losses, the correlation between the freezing date and air temperature becomes high. The average air temperatures of EKK and HIRLAM for the period 15 Oct.–15 Nov. were –0.58 °C and –0.67 °C, respectively. The modelled freezing date in the experiment M1F1 was half day later than that in the experiment M1F2.

The freezing date given by FLake is physically correct, resulting from cooling of the lake waterbody due to surface heat losses. It strongly depends on the water depth. FLake runs gave quite accurate results, except in the experiment M3F2 (no orography correction for air temperature). The freezing date of FLake would be 23 days delayed as compared with that in the experiment M2F1 if the depth of the lake were increased from 20 to 50 m.

The cooling of water due to snowfall is not included in the models. In the climatology of Kilpisjärvi, the mean heat loss in ice-free water due to snowfall is less than 5 W m^{-2}, but in weather forecasting the influence can be significant, on the order of 100 W m^{-2} during a heavy snowfall.

The HIGHTSI ice-breakup date was predicted reasonably well. There were two factors that caused a postponed breakup in HIRLAM run M1F2. A lower air temperature in June as compared with the EKK data and snow-ice formation, which increased the total amount of ice and delayed the onset of ice melting. Water depth has little influence on the ice-breakup date because the surface heat balance dominates the melting of snow and ice.

Unless the lake is small, the freezing and ice-breakup dates may differ due to different definitions (Palecki and Barry 1986). It may last days or weeks from the initial freezing close to the shoreline to the fully ice-covered lake. The same problem also concerns the ice-breakup date (Howell *et al*. 2009), since that also depends on ice mechanics (ice breakage and wind drift). For an accurate detection of freezing and ice-breakup dates, remote sensing technology is a very useful tool (Duguary *et al*. 2003).

Discussion

The ice thicknesses modelled by HIGHTSI and FLake were comparable. The differences were more pronounced during the melting season due to different model physics (*see* Appendix). Overall, HIGHTSI (experiments M1F1 and M1F2) and FLake (experiments M2F1, M2F2 and M3F1) modelled the seasonal snow and ice thicknesses well. The correlation coefficients between modelled and measured snow and ice thicknesses were very high. Experiment M3F2 demonstrated the importance of the orography correction.

The snow thickness measurements at the EKK and 'Lotus' stations showed large temporal variations (Fig. 2). Many factors — snowdrift, morphology of the surrounding area (mountain, hill, or plain), etc. — can affect snow distribution on a lake ice surface. An area-averaged snow thickness is more representative than a single point measurement to be compared with a model result, and a validation of the changes of modelled snow thickness is more meaningful than the absolute level. Previous work has indicated that a prescribed snow density based on measurements can indeed improve overall modelled snow thickness (Semmler *et al*. 2012).

The surface temperature is the main linkage between the atmosphere and the lake below. It affects the structure and stability of the atmospheric boundary layer, turbulent and radiative fluxes, and the conductive heat flux from the lake. The temporal variability in the surface temperature is caused by strong diurnal cycles

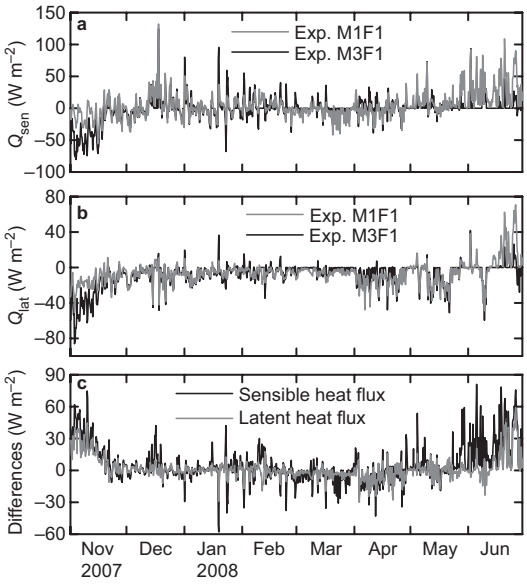

Fig. 10. (**a**) Sensible and (**b**) latent heat fluxes calculated by M1F1 and M3F1, and (**c**) differences between the fluxes in the two models.

or synoptic variations. For a stable atmospheric boundary layer, turbulent fluxes are usually very small and the surface heat balance depends mostly on radiative fluxes. As a result, the surface temperature may decrease very rapidly that may not be captured by NWP models, resulting in large warm bias in the simulations (Marko *et al*. 2007).

For the coupling between the atmosphere and lake, it is interesting to examine the turbulent heat fluxes in more detail (Fig. 10). In the early ice season, FLake gave much stronger sensible and latent heat losses than HIGHTSI, likely due to biased surface temperature in FLake. As soon as the ice cover appears, turbulent fluxes decrease remarkably (Leppäranta *et al*. 2012). At the end of the ice season, turbulent fluxes were too high in HIGHTSI, especially so with the high positive latent heat fluxes. For most of the ice season, the difference between HIGHTSI and FLake modelled turbulent fluxes were on the average 5.46 and 1.68 W m^{-2} for sensible heat and latent heat, respectively. Apart from a short transient occasion, FLake has clearly too much power at very high frequencies caused by its quasi-steady approach to the heat flux through ice and snow.

Conclusions

Snow and ice thermodynamics was investigated by the HIGHTSI and FLake models for an Arctic lake, Kilpisjärvi. HIGHTSI is a high-resolution, time-dependent snow and ice model and FLake is a thermodynamic lake model with a quasi-steady, two-layer (snow + ice) model on top. FLake ignores the heat capacity of snow and ice. The models were driven by the local weather station data and by output of a numerical weather prediction model (HIRLAM). Six model experiments were carried out using different forcing fields and for FLake also two different modes (Standalone and SURFEX-FLake). The results were compared with *in-situ* routine measurements of the ice and snow thicknesses and surface temperature.

The modelled snow and ice thicknesses from HIGHTSI and FLake showed very good agreements with observations, and the differences between the models were small. The onset of ice melting was delayed in both models likely due to albedo parameterizations. The lowest absolute errors between the observed and simulated ice thickness were 5.95 cm (SURFEX-FLake) and 7.29 cm (HIGHTSI) forced by EKK and HIRLAM, respectively, only with a 1.3 cm bias. The snow thickness was predicted less accurately, in particular for the melting season. Snow thickness could be validated from the data on lake ice, and it was found that it differed from that at the site on land (EKK weather station) by as much as 50 cm. For the ice thickness and surface temperature, the snow cover is critically important. HIGHTSI does not include lake waterbody and cannot predict the freezing date properly, while FLake predicted it well. The ice-breakup date modelled by HIGHTSI and FLake differed a little from each other.

HIRLAM can provide reasonable boundary conditions to drive HIGHTSI and FLake. The seasonal HIRLAM wind was on average 1.7 m s^{-1} faster than the measured values. In stable atmospheric stratification, HIRLAM seemed to overestimate air temperature up to about 4 °C. In winter, HIRLAM can provide snowfall that is comparable with the local measurements. In warm conditions, however, the total precipitation is greater than the recorded. Orography correc-

tion of HIRLAM air temperature is very important. The difference in solar radiation between the measurements and predictions by HIRLAM was about 10%.

The surface temperature modelled by both HIGHTSI and FLake was warm-biased, typically so for a stable atmospheric boundary layer. For FLake, the bias was smaller than for HIGHTSI, because there were compensating errors, but the RMSE was larger in FLake than in HIGHTSI. Both models had errors in amplitude and in phase, in particular they were not able to reproduce rapid changes. These errors may originate from numerical reasons (temporal resolution, implicit scheme) in HIGHTSI, and from the quasi-steady approach and resolution in FLake that will be a topic of a future study. Calculation of the surface temperature with a direct method is cost effective and largely used in NWP models. According to our case study, iterative methods could increase the accuracy by about 0.3–0.4 °C. Thus improving computing capacity does have a potential to increase the performance of numerical weather forecasting by coupling lake-ice models with NWP models. In December–February, the difference between the air and surface temperatures was often greater than 5 °C. In the melting season, the modelled and measured surface temperatures were close to 0 °C and therefore the error was small.

Provided with good atmospheric forcing, FLake reproduces the main features of snow and ice thermodynamics, including the freezing and ice-breakup dates, quite well. It is also widely used in NWP models. But due to the two-layer approach (i.e. low vertical resolution), it is difficult for FLake to reproduce the detailed time evolution of snow and ice surface temperature. HIGHTSI works better for this, but still further research is needed to reproduce high frequency variations. HIGHTSI would have a strong potential for improvements if it were included as a module in SURFEX, which is used in many environmental applications. For NWP and climate modelling, further research is needed to achieve a good compromise between the lake-ice model resolution and computational efficiency, as well as to solve the lake-ice and snow initialization problem.

Acknowledgements: The Kilpisjärvi Biological Station and the Finnish Environment Institute (SYKE) are thanked for the data. This research was supported by the Natural Science Foundation of China (grants 51079021, 40930848 and 50879008), the Norwegian Research Council (grant 193592/S30), the Academy of Finland (140939/Leppäranta), and the Finnish Cultural Foundation (Leppäranta). The first author was supported in 2010 by CIMO scholarship from the Ministry of Education in Finland.

References

Bennett T.J. 1982. A coupled atmosphere–sea–ice model study of the role of sea ice in climatic predictability. *J. Atmos. Sci.* 39: 1456–1465.

Briegleb B.P., Bitz C.M., Hunke E.C., Lipscomb W.H., Holland M.M., Schramm J.L. & Moritz R.E. 2004. *Scientific description of the sea ice component in the Community Climate System Model, version 3*. Tech. Rep. NCAR/TN-463+STR, National Center for Atmospheric Research, Boulder, CO.

Brown L.C. & Duguay C.R. 2010. The response and role of ice cover in lake-climate interactions. *Prog. Phys. Geogr.* 34: 671–704.

Cheng B., Vihma T. & Launiainen J. 2003. Modelling of the superimposed ice formation and sub-surface melting in the Baltic Sea. *Geophysica* 39: 31–50.

Cheng B., Vihma T., Pirazzini R. & Granskog M. 2006. Modelling of superimposed ice formation during spring snowmelt period in the Baltic Sea. *Ann. Glaciol.* 44: 139–146.

Cheng B., Zhang Z., Vihma T., Johansson M., Bian L., Li Z. & Wu H. 2008. Model experiments on snow and ice thermodynamics in the Arctic Ocean with CHINAREN 2003 data. *J. Geophys. Res.* 113, C09020, doi:10.1029/2007JC004654.

Croley T.E.II & Assel R.A. 1994. A one-dimensional ice thermodynamics model for the Laurentian Great Lakes, *Water Resour. Res.* 30: 625–639.

Duguay C.R., Flato G.M., Jeffries M.O., Ménard P., Morris K. & Rouse W.R. 2003. Ice-cover variability on shallow lakes at high latitudes: model simulations and observations. *Hydrol. Proces.* 17: 3464–3483.

Eerola K., Rontu L., Kourzeneva E. & Shcherbak E. 2010. A study on effects of lake temperature and ice cover in HIRLAM. *Boreal Env. Res.* 15: 130–142.

George D.G., Järvinen M. & Arvola L. 2004. The influence of the North Atlantic Oscillation on the winter characteristics of Windermere (UK) and Pääjärvi (Finland). *Boreal Env. Res.* 9: 389–399.

Goyette S., McFarlane N.A. & Flato G.M. 2000. Application of the Canadian regional climate model to the Laurentian great lakes region: implementation of a lake model. *Atmosphere-Ocean* 38: 481–503.

Hanna S.R. & Yang R. 2001. Evaluation of mesoscale numerical models' simulations of near surface wind, temperature gradients and mixing depth. *J. Appl. Meteor.* 40: 1095–1104.

Heron R. & Woo M.K. 1994. Decay of a High Arctic lake-ice cover: observations and modelling. *J. Glaciol.* 40: 283–292.

Hodgkins G.A., James I.C. & Huntington T.G. 2002. Historical changes in lake ice-out dates as indicators of climate change in New England, 1850–2000. *Int. J. Climatol.* 22: 1819–1827.

Hostetler S.W., Bates G.T. & Giorgi F. 1993. Interactive coupling of a lake thermal model with a regional climate model, *J. Geophys. Res.* 98: 5045–5057.

Howell S.E.L., Brown L.C., Kang K.K. & Duguay C.R. 2009. Variability in ice phenology on Great Bear Lake and Great Slave Lake, Northwest Territories, Canada, from SeaWinds/QuikSCAT: 2000–2006. *Remote Sens. Environ.* 113: 816–834.

Järvenoja S. 2005. Problems in predicted HIRLAM T2m in winter, spring and summer. *Proceedings of the SRNWP/HIRLAM Workshop on Surface Processes and Turbulence*, SMHI, Norrköping, 15–17 September 2004, pp. 14–26.

Launiainen J. & Cheng B. 1998. Modelling of ice thermodynamics in nature water bodies. *Cold Reg. Sci. Technol.* 27: 153–178.

Lei R., Leppäranta M., Cheng B., Li Z. & Heil P. 2012. Changes of ice-season characteristics in an Arctic lake from 1964 to 2008. *Climatic Change* 115: 725–739.

Lei R., Leppäranta M., Erm A., Jaatinen E. & Pärn O. 2011. Field investigations of apparent optical properties of ice cover in Finnish and Estonian lakes in winter 2009. *Est. J. Earth Sci.* 60: 50–64.

Leppäranta M. 1983. A growth model for black ice, snow ice and snow thickness in subarctic basins. *Nordic Hydrology* 14: 59–70.

Leppäranta M. 2009. Modelling the formation and decay of lake ice. In: George D.G. (ed.), *The Impact of Climate Change on European Lakes*, Aquatic Ecology Series 4, Springer Science+Business Media B.V., pp. 63–83.

Leppäranta M. & Lewis J.E., 2007. Observations of ice surface temperature in the Baltic Sea. *International Journal of Remote Sensing* 28: 3963–3977.

Leppäranta M., Shirasawa K. & Takatsuka. T. 2012. Ice season in Lake Kilpisjärvi in Arctic tundra. In: Li Z. & Lu P. (eds.), *Proceedings of the 21st IAHR International Symposium on Ice*, Dalian University of Technology, Dalian, China, paper no. 115.

Leppäranta M. & Uusikivi J. 2002. The annual cycle of the Lake Pääjärvi ice. *Lammi Notes* 29: 4–9.

Le Moigne P. 2009. *SURFEX scientific documentation*. Note de centre (CNRM/GMME), Météo-France, Toulouse.

Magnuson J.J., Robertson D.M., Benson B.J., Wynne R.H., Livingstone D.M. & Arai T. 2000. Historical trends in lake and river ice cover in the northern hemisphere. *Science* 289: 1743–1746.

Marko M., Hsieh C., Schalek R., Frank J. & Mannella C. 2007. Focused-ion-beam thinning of frozen-hydrated biological specimens for cryo-electron microscopy. *Nat. Methods* 4: 215–217.

Mironov D.V. 2008. *Parameterization of lakes in numerical weather prediction. Description of a lake model*. Technical Report of COSMO no. 11, Deutscher Wetterdienst, Offenbach am Main.

Mironov D., Heise E., Kourzeneva E., Ritter B., Schneider N. & Terzhevik A. 2010. Implementation of the lake parameterization scheme FLake into the numerical weather prediction model COSMO. *Boreal Env. Res.* 15: 218–230.

Palecki M.A. & Barry R.G. 1986. Freeze-up and break-up of lakes as an index of temperature changes during the transition seasons: A case study for Finland. *J. Appl. Meteorol. Climatol.* 25: 893–902.

Patterson J.C. & Hamblin P.F. 1988. Thermal simulation of a lake with winter ice cover. *Limnol. Oceanogr.* 33: 323–338.

Salgado R. & Le Moigne P. 2010. Coupling of the FLake model to the Surfex externalized surface model. *Boreal Env. Res.* 15: 231–244.

Saloranta T. 2000. Modelling the evolution of snow, snow ice and ice in the Baltic Sea. *Tellus* 52A: 93–108.

Semmler T., Cheng B., Yang Y. & Rontu L. 2012. Snow and ice on Bear Lake (Alaska)-sensitivity experiments with two lake ice models. *Tellus* 64A, 17339, doi:10.3402/tellusa.v64i0.17339.

Shine K.P. 1984. Parameterization of shortwave flux over high albedo surfaces as a function of cloud thickness and surface albedo. *Quart. J. Roy. Meteor. Soc.* 110: 747–764.

Sturm M., Holmgren J., König M. & Morris K. 1997. The thermal conductivity of snow. *J. Glaciol.* 43: 26–41.

Undén P., Rontu L., Järvinen H., Lynch P., Calvo J. & coauthors. 2002. *The HIRLAM-5 scientific documentation*. SMHI, Sweden, [available at http://hirlam.org].

Yang Y., Leppäranta M., Cheng B. & Li Z. 2012. Numerical modelling of snow and ice thickness in Lake Vanajavesi, Finland. *Tellus* 64A, 17202, doi:10.3402/tellusa.v64i0.17202.

Yen Y.C. 1981. Review of thermal properties of snow, ice and sea ice. *Cold Regions Research and Engineering Laboratory (CRREL) Report* 81-10, Hanover, NH, pp. 1–27.

Zhou X., Li S. & Stamnes K. 2003. Effects of vertical inhomogeneity on snow spectral albedo and its implication for optical remote sensing of snow. *J. Geophys. Res.* 108(D23), 4738, doi:10.1029/2003JD003859.

Appendix

A detailed comparison of the HIGHTSI and FLake models for snow and ice physics with the model parameters are shown in Tables A1 and A2. h_{snow}, h_{ice} and h_w are the snow thickness, ice thickness and mean lake depth, respectively; "+" and "–" mean growth and decay; T_{snow}, T_{ice} and T_w are temperatures of snow, ice and water, respectively; α is albedo; I_0 is the portion of solar radiation penetrating below the surface layer, Q_b is the outgoing long-wave radiation; F_c is the surface conductive heat flux, and F_m is the latent heat flux due to fusion. T_f is the ice–water interface temperature, and F_w is the heat flux from water to ice bottom. Detailed description of the HIGHTSI and FLake models can be found in Cheng *et al*. (2003) and Mironov *et al*. (2010).

Table A1. Snow and ice thermodynamic processes in HIGHTSI and FLake.

	HIGHTSI	FLake
Model	1D snow and ice model	1D lake model with snow and ice layers on top
Main thermal processes in snow and ice	Time dependent heat conduction and radiation transfer	Quasi-steady heat flux, radiation transfer, heat flux from water
External forcing	Wind, air temperature, humidity, cloudiness, precipitation, solar radiation	
Initial condition	h_{snow}, h_{ice}, T_{snow}, T_{ice}	h_{snow}, h_{ice}, T_{snow}, $T_{ice,}$ T_w, h_w
Boundary conditions		
Surface heat balance	$(1-\alpha_{snow,ice})Q_s - I_0 + Q_d + Q_b + Q_h + Q_{le} + F_c - F_m = 0$	
Surface temperature	Iterative method	Non-iterative
Ice–water interface	Temperature 0 °C Constant heat flux from water (based on function of ice concentration)	Temperature 0 °C Heat flux from water to ice calculated by the model
Freezing date	Surface heat balance	Surface heat balance and mixing of the surface water layer
Snow		
h_{snow}	Precipitation (+), melting of surface and subsurface (–), refreezing of slush (–), and metamorphosis	Precipitation (+) and snowmelt at surface (–)
T_{snow}	Solve heat conduction equation, implicit scheme, time-dependent	Solve heat conduction equation, explicit scheme, quasi-steady
Ice		
h_{ice}	Freezing (+), melting of surface and subsurface (–), snow-ice (+), superimposed ice (+)	Freezing (+), melting (–)
T_{ice}	Solve heat conduction equation, implicit scheme, time-dependent	Solve heat conduction equation, explicit scheme, quasi-steady

Table A2. Model physical parameters used in HIGHTSI and FLake.

Parameter	Value	
	HIGHTSI	FLake
Time step (s)	3600	3600
Spatial resolution (number of layers)	10 (snow), 20 (ice)	4 (snow + ice + mixed layer + thermocline)
Lake ice density (kg m^{-3})	910	910
Snow density assumed to convert precipitation (water equivalent) to snow depth (kg m^{-3})	320, Zhou *et al.* (2003)	
Snow-ice density (kg m^{-3})	850	–
Thermal conductivity of ice (W m^{-1} K^{-1})	2.03, Yen (1981)	2.29
Thermal conductivity of snow (W m^{-1} K^{-1})	Sturm *et al.* (1997)	Semmler *et al.* (2011)
Extinction coefficient of lake ice (m^{-1})	1.5–17 (Heron *et al.* 1994, Lei *et al.* 2011)	–
Extinction coefficient of snow (m^{-1})	6–20 (Patterson *et al.* 1988, Lei *et al.* 2011)	–
Freezing temperature (°C)	0	0
Heat capacity of ice (J kg^{-1} K^{-1})	2093	2100
Surface emissivity	0.97	0.99
Heat flux from water (W m^{-2})	1.5	Given by FLake
Latent heat of freezing (J kg^{-1})	0.33×10^6	
Surface albedo	Snow/ice thickness; temperature and spectral dependent (Briegleb *et al.* 2004)	0.50 (white ice); 0.30 (blue ice), 0.87 (dry snow); 0.77 (wet snow) (Semmler *et al.* 2011)